Energy-Efficient SWIPT-Empowered D2D Mode Selection

Jun Huang, *Senior Member, IEEE,* Jingjing Cui, Cong-cong Xing and Hamid Gharavi, *Life Fellow, IEEE*

***Abstract*—While mode selection has been envisioned as the most cost-effective way to address the interference issue in Device-to-Device (D2D) communications, existing works have been largely conducted without consideration of the energy depletion of devices. In this paper we investigate simultaneous wireless information and power transfer (SWIPT) empowered mode selection based on stochastic geometry. As a mean of solving it, system energy efficiency is formulated by determining the closed-form ergodic energy-harvested and ergodic capacity of D2D and cellular users in reuse, dedicated, and cellular communication modes with the time switching and power splitting architectures of SWIPT. We then leverage the derived results, along with the energy efficiency to design an energy-efficient mode selection mechanism. Our simulation results show that the developed mechanism is able to select the best mode for D2D communication with better energy efficiency, especially in an ultra-dense cellular network as compared with a state-of-the-art mode selection approach.**

***Index Terms*—simultaneous wireless information and power transfer, mode selection, power splitting, time switching, energy efficiency.**

I. Introduction

A. Background

WHILE interference management [1]–[4], plays a critical role in implementing Device-to-Device (D2D) communications in cellular networks, mode selection [5]–[8], has been realized as the most useful means. The aim is to select one of the following three communication modes; reuse, dedicated, and cellular. In the reuse mode, D2D communications are carried out by letting D2D users reuse the cellular uplink resources at the expense of possible interference between D2D links and the reused cellular links. On the other hand, the dedicated mode requires certain spectrum resources, which are solely reserved for D2D users by the base station. In this case there would be no interference between D2D links and cellular links. In cellular mode, D2D users act just like cellular users and the base station serves as a relay to transfer data between D2D transmitters and receivers. Also, in this mode there would be no interference between D2D and cellular communications. In general, the interference experienced by D2D and cellular users is not the same as in different modes, which leads to a varying system performance.

Another crucial issue in D2D communication lies in the Energy Efficiency (EE) [9]–[11]. This is attributed to the fact that the unprecedented growth of mobile users, mobile apps, and real-time Internet traffic, is intensifying network energy consumption, thus causing rapid battery depletion in mobile devices. A closely related technique that addresses the EE issue, is Simultaneous Wireless Information and Power Transfer (SWIPT) [12]–[14]. SWIPT allows the energy to be harvested by devices to which data is being transferred. As such, undertaking SWIPT in D2D communications enables D2D and cellular devices to harvest energy during the process of data transfer, which can be very beneficial in prolonging the standby time of devices and enhancing the EE of the system [15]–[19].

As the position of a mobile device is random, a new challenge associated with mode selection (when SWIPT meets D2D communications) is how to model and analyze the energy harvesting of mobile devices in order to enable energy-efficient SWIPT-empowered mode selection. Stochastic geometry has been established as a powerful tool in tackling randomness issues in wireless networks [17]. Specifically, both the legitimate signal power and the interference power can be regarded as random processes due to the mobility nature of transmitters, which can impact the channel fading conditions of the transmission path. Under these conditions, the stochastic geometry can play a major role in computing the statistical properties of energy harvesting that can effectively contribute to the D2D mode selection mechanism thereby improving the energy efficiency in the presence of SWIPT.

B. Related Work

Currently, extensive research efforts have been carried out is that dedicated to interference management and system throughput maximization in D2D mode selection and energy harvesting. Sakr et al. [20] proposed a new cognitive D2D communication model that uses radio frequency (RF) energy harvesting from interference and used stochastic geometry to analysis the performance of the proposed system based on D2D and cellular users transmission probability and SINR outage probabilities. In [21], the authors analyzed the spectral efficiency and coverage probability of D2D-assisted Machine-type communications under spatially correlated interference, and used spectral efficiency to study the impact of RF energy harvesting on the systems performance. However, the channel gain of the D2D link in these two papers is subject to Rayleigh

J. Huang is with the School of Commu. and Info. Eng. and the School of Computer Science, Chongqing University of Posts and Telecom, Chongqing, 400065 China, e-mail: huangj@ieee.org

J. Cui is with the School of Commu. and Info. Eng., Chongqing University of Posts and Telecom, Chongqing, 400065 China, e-mail:cuijj0315@gmail.com

C. Xing is with the Department of Mathematics and Computer Science, Nicholls State University, Thibodaux, 70310 USA, e-mail: cong-cong.xing@nicholls.edu.

H. Gharavi is with the National Institute of Standards and Technology, Gaithersburg, 20855 USA, E-mail: hamid.gharavi@nist.gov.

fading. Kuang et al. [22] investigated the DUEs multiplexing CUEs downlink spectrum resources problem for EH-based D2D communication heterogeneous networks, the D2D and cellular users energy harvested is directly assumed to be a Poisson point process, which does not match the actual. In [23], authors explored the mean value of system capacity for both cellular and D2D links, and devised two energy-efficient mode selection mechanisms based on the system energy efficiency.

The limitation of battery lifetime and the ensuing SWIPT remedy for it is also well-investigated. For instance, Mohjazi et al. [24] evaluated the system throughputs under the time switching (TS) and power splitting (PS) architectures for a relatively low SNR. They use outage probability and harvested energy to study differential modulation in SWIPT relay networks. Subsequently, Mohjazi et al. [25] also studied the system performance of SWIPT relay networks with noncoherent modulation. They conclude that under the conditions of lower SNR and maximized system throughput, the performance of the TS protocol exceeds that of the PS protocol. The performance of the TS-based SWIPT in a wireless network was evaluated in [26] using a Non-Orthogonal Multiple Access (NOMA) technique. In addition, Zwede and Gursoy [27] investigated a wireless network scenario consisting of randomly deployed access points and SWIPT-empowered user equipment. In [28], the authors propose a SWIPT-based traffic offloading scheme, the traffic offloading via D2D communications was utilized to alleviate the heavy burden on the capacity-limited front hauls, while the energy harvesting design is adopted to stimulate offloading by compensating the energy consumption at the D2D transmitters. Their main focus has been to optimize system throughput and energy efficiency by formalizing the outage probability and achievable data rate as functions of system parameters. Furthermore, Stochastic geometry was applied to characterize cell load statistics at the macrocell base stations (MBSs) and small cell BSs (SBSs), as well as summary information and interference signal strength in [29]. In this way, the average user capacity of the joint transmission was obtained. Khanet et al. [30] consider a large-scale cooperative wireless network and provide a tractable analytical framework to describe the link and network-level performance at the receiver amid heterogeneous network interference.

C. Motivation and Contribution

Previous studies in D2D mode selection are primarily focused on interference management and EE, which do not take SWIPT into account [5], [6], [9], [23]. As explained, the lifetime of mobile devices will be significantly prolonged by SWIPT, redesigning mode selection mechanism for SWIPT-enabled D2D communications is of particular importance. Also, existing computation in current works cannot be transplanted into SWIPT-empowered D2D communications, because, the analysis of EE in the presence of SWIPT is not the same as in previous results. Hence, a new analytical tool is needed. Although the theory of stochastic geometry is leveraged to calculate the energy harvested by [22], its underlying assumption of energy harvesting following the Poisson Point Process (PPP) is not practical as various random factors will distort such a process. In other words, the calculation of EH in [22] is imprecise.

In this paper, we apply stochastic geometry to SWIPT-empowered D2D communications and design a mode selection mechanism. The contributions made in this paper are summarized as follows:

- We analyze the energy harvested by D2D users and cellular users leveraging stochastic geometry (SG) under the TS and PS architectures of SWIPT, and obtain the closed-form expression of the *ergodic energy-harvested* (EEH). As we know, this work is one of the early attempts on analysis of energy harvesting by SG.
- With the analyses of EEH and ergodic capacity, the system EE is then investigated in a different mode. A mode selection mechanism based on the system EE is designed, which can determine the optimal D2D communication mode in reducing energy consumption of the system, as well as enhancing the standby time of devices.
- The effectiveness of the proposed mode selection mechanism is demonstrated via extensive simulations. The results show that our mechanism is able of selecting the best mode for D2D communication with better EE, especially in an ultra-dense cellular network, compared with the state-of-the-art mode selection approach.

D. Roadmap

The rest of the paper is structured as follows; Section II introduces the system model. In Section III, we tackle the amount of SWIPT-harvested energy by D2D users and cellular users in three D2D communication modes. Section IV presents calculations of the ergodic capacity of D2D and cellular links. Section V presents the mode selection mechanism. Section VI describe and analyzes the simulation results before presenting the final remarks and conclusion in Section VII.

II. System Model

For our model, we consider a multiple cells scenario, where a cellular user is restricted to communicate with the nearest base station, a D2D user can work either in reuse or dedicated or cellular mode as shown in Fig. 1. In this scenario, we characterize a set of: cellular users ($\mathbf{C}$), D2D users ($\mathbf{D}$, either D2D transmitters or receivers), and base stations ($\mathbf{B}$), as Poisson point processes (PPP); Φ_C, Φ_D, and Φ_B with densities λ_C, λ_D, and λ_B, respectively. We also assume that d_C corresponds to a distance between a cellular user and a base station and d_D represents the distance between a pair of D2D user equipment. Then, according to PPP, the probability density functions (pdf) of the cellular user and the D2D link can respectively be shown as:

$$f_C(d_C) = 2\pi\lambda_B d_C \exp(-\pi\lambda_B {d_C}^2) \tag{1}$$

and

$$f_D(d_D) = 2\pi\lambda_D d_D \exp(-\pi\lambda_D {d_D}^2). \tag{2}$$

It should be noted that the transmit power of any cellular user depends on its distance to the base station, which varies

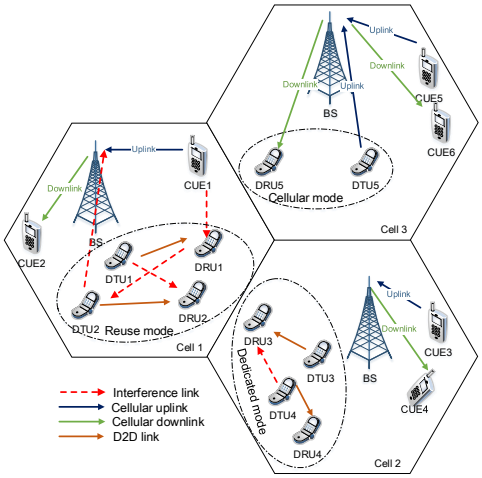

Fig. 1: An illustrative system scenario (DTU = D2D transmitter, DRU = D2D receiver, CUE = cellular user, BS = base station).

from one user to another. As such, each cell, we stratify all cellular users into s (s is a variable) tiers that is, cellular users located in the same tier have an identical transmit power. Let $C_{\gamma,i}$ denote the i-th cellular user at the γ-th tier, where $(\gamma = 1, 2, \ldots, s)$, and P_{C_γ} ($P_{C_\gamma} \neq P_{C_\delta}$ if $\gamma \neq \delta$) represent the transmit power of cellular users at the γ-th tier. Furthermore, we assume that the transmit power of each D2D link is P_D under reuse and dedicated modes. This is based on the assumption that distances from any D2D transmitter to its receiver are relatively short under these two communication modes. In the cellular mode, however, we mark it as P_{D_γ} if the D2D user is located at tier γ (as any D2D user in this communication mode would be treated like regular cellular users, and thus be stratified as well). For the base station in each cell, we assume that it's transmit power P_B is fixed during data transmission process.

Power Splitting (PS) and Time Switching (TS) are two essential components that enable SWIPT implementation. In the PS architecture, a portion of the total received power at a device is used to decode information and the rest is used for harvesting energy. In the TS architecture, received signals are used for energy-harvesting during a certain time period within a receiving cycle. They are used for information-decoding for the remaining cycle time. Note that both architectures aim at compensating the energy consumption of devices, and thereby enhance their standby time by means of harvesting energy. As such, the working procedure of SWIPT can consist of an energy harvesting stage and data transfer stage. In the former, the amount of energy harvested by D2D users in different modes can change due to a different amount of interference experienced by D2D users in each mode. Specifically, in cellular communication mode, D2D and cellular users can only harvest energy from the base station's downlinks. In the data transfer stage, the spectrum available for a cell is divided into sub-spectrums that are designated for cellular users. Under these conditions, D2D users are allowed to reuse available uplink resources of cellular users (under reuse communication mode). In the dedicated communication mode, only a fixed portion of the spectrum will be reserved for D2D communications and the remaining spectrum will be available for cellular users. In the cellular communication mode, D2D users act just like cellular users using the base station to transfer data.

As far as system interference is concerned, since D2D users reuse the uplink spectrum resources of cellular users (under the reuse communication mode), they are subject to both intra- and inter-cell interferences caused by other D2D users and/or cellular users. At the same time, cellular users will experience interference by intra- and inter-cell D2D users, and intra-cell cellular users. Under dedicated and cellular communication modes, however, D2D users and cellular users do not interfere with each other.

Regarding channel gain, we stipulate that D2D links follow *Rician* fading with path loss $d_D^{-\alpha}$ in reuse or dedicated mode and *Rayleigh* fading with path loss $d_C^{-\alpha}$ (α is the path loss component) in cellular mode. The reason for this assumption is that the distance from a DTU to a DRU is relatively short and can likely be within a line-of-sight (LoS) in both reuse and dedicated modes and a non-line-of-sight (NLoS) likelihood in cellular mode due to longer distances. Analogously, the channel gain of the interference links; CUE-DRU (from CUE to DRU), DTU-DRU, and BS-DRU, all follow *Rayleigh* fading since they are all NLoS. We put the frequently used symbols and notations in Table I, which is located in Section VI.

In light of the above assumptions, in the following sections, we will first analyze the energy harvesting of both cellular and D2D users; and then combine these analytical results with those of the system capacity to design a mode selection mechanism on the basis of system EE.

III. Analysis of Energy-Harvesting

To analyze the energy harvesting of D2D and cellular users, we devise a new metric, termed *Ergodic Energy-Harvested* (EEH), to reflect the amount of energy collected at receivers under the time switching (TS) and power splitting (PS) architectures of SWIPT.

A. EEH under TS Architecture

For the TS architecture, we assume that over the total amount of time; T, its τT $(0 \leq \tau \leq 1)$ portion will be used for energy harvesting and the rest: $(1-\tau)T$, will be allocated for information decoding, as shown in Fig. 2. Note that when the receiver is engaged in energy harvesting (i.e., during; τT), no data transfer activity will occur.

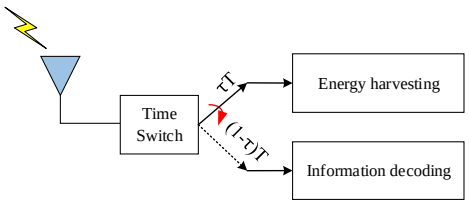

Fig. 2: Time Switching Architecture of SWIPT.

1) EEH for D2D Users: D2D users collect energy from the base station. Let $l_{B_k,D_{a'}}$ be the downlink from base station; B_k, to DRU; $D_{a'}$, then the received power at $D_{a'}$ would be $S_D = P_{B_k} d^{-\alpha}_{B_k,D_{a'}} h_{B_k,D_{a'}}$, where P_{B_k} is the transmit power of base station B_k, $d_{B_k,D_{a'}}$ is the distance from the base station B_k to the DRU $D_{a'}$, and $h_{B_k,D_{a'}}$ is the channel gain of link. Note that $l_{B_k,D_{a'}}$ having an exponential distribution with mean value 1 (i.e., $h_{B_k,D_{a'}} \sim \exp(1)$) by virtue of [23]. Given this setting, we have the following theorem.

Theorem 1: Under the TS architecture, the ergodic energy harvested at the DRU $D_{a'}$ for the downlink $l_{B_k,D_{a'}}$ is:

$$\mathrm{EEH}_{B_k,D_{a'}} = \tau\eta P_{B_k}\left[\hat{d}^{-\alpha}(-e^{-\pi\lambda_B\hat{d}^2}+1)+ (\pi\lambda_B)^{\alpha/2}\,\Gamma\left(\frac{-\alpha+2}{2},\pi\lambda_B\hat{d}^2\right)\right], \tag{3}$$

where η is the energy conversion efficiency, τ is the percentage of time for energy harvesting in the TS architecture, $\hat{d} \geq 1$ is used to avoid modeling inaccuracy for very short distance [27], [31], and $\Gamma(v,z) = \int_z^{+\infty} u^{v-1}e^{-u}du$ is the incomplete gamma function.

Proof: See Appendix A. ∎

2) EEH for Cellular Users: Analogous to D2D users, cellular users harvest energy from the base station as well. For any cellular downlink; $l_{B_k,C_{\gamma,i}}$, the power received at a cellular user; $C_{\gamma,i}$ would be $S_C = P_{B_k} d^{-\alpha}_{B_k,C_{\gamma,i}} h_{B_k,C_{\gamma,i}}$, where $C_{\gamma,i}$ is the i-th cellular user at the tier γ, P_{B_k} is the transmit power of base station; B_k, $d_{B_k,C_{\gamma,i}}$ is the distance from B_k to $C_{\gamma,i}$, and $h_{B_k,C_{\gamma,i}}$ is the channel gain of link $l_{B_k,C_{\gamma,i}}$ which is of an exponential distribution with mean value 1 (i.e., $h_{B_k,C_{\gamma,i}} \sim \exp(1)$). Accordingly, the energy harvested at cellular user $C_{\gamma,i}$ is similar to the energy harvested at the DRU for a D2D downlink.

Theorem 2: Under the TS architecture, the energy harvested at the cellular user $C_{\gamma,i}$ for the cellular downlink $l_{B_k,C_{\gamma,i}}$ can be shown as:

$$\mathrm{EEH}_{B_k,C_{\gamma,i}} = \tau\eta P_{B_k}\left[\hat{d}^{-\alpha}\left(-e^{-\pi\lambda_B\hat{d}^2}+1\right)+ (\pi\lambda_B)^{\alpha/2}\,\Gamma\left(\frac{-\alpha+2}{2},\pi\lambda_B\hat{d}^2\right)\right], \tag{4}$$

where all the notations have the same meaning as in Eq. (3).

Proof: Follow the similar lines of Theorem 1's proof. ∎

Theorem 1 and Theorem 2 simply indicate that: the larger transmit power of BS or the larger density of BS or the longer time for energy harvesting in the TS architecture of SWIPT, the more energy being harvested at receivers.

B. EEH under PS Architecture

The PS architecture of SWIPT where the received signal power (P) is split into two streams: with one κP being used for energy harvesting and the other $(1-\kappa)P$ for information decoding, as shown in Fig. 3. Below, we discuss energy harvesting for D2D users and cellular users under the reuse, dedicated, and cellular communication modes, separately.

1) EEH for D2D Users:

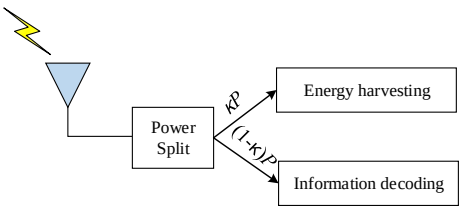

Fig. 3: Power Splitting Architecture of SWIPT.

a) In Reuse Mode: For any D2D link $l_{D_a,D_{a'}}$ in reuse mode with D_a being the transmitter and $D_{a'}$ being the receiver, the signal power received at $D_{a'}$ is $S_D = P_D d^{-\alpha}_{D_a,D_{a'}} g_{D_a,D_{a'}}$, where P_D is the transmit power of D_a, $d_{D_a,D_{a'}}$ is the distance between D_a and $D_{a'}$, and $g_{D_a,D_{a'}}$ is the signal fading from D_a to $D_{a'}$. Note that $g_{D_a,D_{a'}}$ is a *Rician* fading and follows a non-central χ^2 distribution with *Rician* factor K (the ratio of direct power to scattered power). The pdf of $g_{D_a,D_{a'}}$ is $f_{g_{D_a,D_{a'}}}(g) = \frac{(K+1)e^{-K}}{\bar{g}} \exp\left(-\frac{(K+1)g}{\bar{g}}\right) I_0\left(\sqrt{\frac{4K(K+1)g}{\bar{g}}}\right)$, where $\bar{g}$ is the mean, and $I_0(\cdot)$ is the zero-order Bessel function. Note that when the scattered power is 0.5, the mean would be $\bar{g}{=}K+1$ and the pdf of $g_{D_a,D_{a'}}$ reduces to $f_{g_{D_a,D_{a'}}}(g) = \exp(-K-g)\sum_{k=0}^{\infty}\frac{(Kg)^k}{(k!)^2}$. Also, for this D2D link; $l_{D_a,D_{a'}}$, the interference power experienced at $D_{a'}$ is $I = I_{\mathbf{C},D_{a'}} + I_{\mathbf{D}_{-a},D_{a'}}$ with $I_{\mathbf{C},D_{a'}} = \sum_{j=1}^{s}\sum_{C_{j,i}\in\mathbf{C}} P_{C_j} d^{-\alpha}_{C_{j,i},D_{a'}} h_{C_{j,i},D_{a'}}$ and $I_{\mathbf{D}_{-a},D_{a'}} = \sum_{D_{a''}\in\mathbf{D}_{-a}} P_D d^{-\alpha}_{D_{a''},D_{a'}} h_{D_{a''},D_{a'}}$, where $\mathbf{D}_{-a} = \mathbf{D} - \{D_a\}$, P_{C_j} is the transmit power of cellular users at tier j, $C_{j,i}$ denotes the cellular user i at tier j, $d_{C_{j,i},D_{a'}}$ is the distance from cellular user $C_{j,i}$ to D2D user $D_{a'}$, and both $h_{C_{j,i},D_{a'}}$ and $h_{D_{a''},D_{a'}}$ are channel gains of the link $l_{D_a,D_{a'}}$ and follow an exponential distribution with mean value 1 (i.e., $h_{C_{j,i},D_{a'}} \sim \exp(1)$ and $h_{D_{a''},D_{a'}} \sim \exp(1)$).

With the above, we have the following results.

Theorem 3: Under the PS architecture and in the reuse mode of D2D communications, for any D2D link; $l_{D_a,D_{a'}}$, the energy harvested at $D_{a'}$ is

$$\mathrm{EEH}_{D_a,D_{a'}} = \kappa\eta\left\{P_D\left[\hat{d}^{-\alpha}\left(-e^{-\pi\lambda_D\hat{d}^2}+1\right)+(\pi\lambda_D)^{\alpha/2}\cdot \Gamma\left(\frac{-\alpha+2}{2},\pi\lambda_D\hat{d}^2\right)\right](1+K)+\sum_{j=1}^{s}P_{C_j}\pi\lambda_C\cdot \hat{d}^{-\alpha+2}\frac{\alpha}{\alpha-2}+P_D\pi\lambda_D\hat{d}^{-\alpha+2}\frac{\alpha}{\alpha-2}\right\}. \tag{5}$$

Proof: See Appendix B. ∎

b) In Dedicated Mode: The difference between the dedicated and the reuse mode in D2D communications is due to the the interference between cellular users and D2D users, which exists in reuse mode, but does not exist in dedicated mode. As such, the energy harvested by D2D users in dedicated mode can be obtained by modifying the counterpart in the reuse mode.

Theorem 4: Under the PS architecture and in the dedicated mode of D2D communications, for any D2D link; $l_{D_a,D_{a'}}$, the energy harvested at $D_{a'}$ is

$$\mathrm{EEH}_{D_a,D_{a'}} = \kappa\eta\left\{P_D\left[\hat{d}^{-\alpha}\left(-e^{-\pi\lambda_D\hat{d}^2}+1\right)+(\pi\lambda_D)^{\alpha/2}\cdot \Gamma\left(\frac{-\alpha+2}{2},\pi\lambda_D\hat{d}^2\right)\right](1+K)+P_D\pi\lambda_D\hat{d}^{-\alpha+2}\frac{\alpha}{\alpha-2}\right\}. \tag{6}$$

Proof: Follow the similar lines of Theorem 3's proof. ■

According to Eq. (5) and Eq. (6), we see that an increased P_D or an increased λ_D will heighten the harvested energy.

c) In Cellular Mode: D2D communications in this mode, just like cellular communications, need to go through the base station. In this mode, energy harvesting occurs only at the DRUs of downlinks with the base station as the transmitter and the D2D user as the receiver. For any downlink $l_{B_k,D_{a'}}$ formed with base station B_k and DRU $D_{a'}$, the signal power received at $D_{a'}$ is $S_D = P_{B_k}d_{B_k,D_{a'}}^{-\alpha}h_{B_k,D_{a'}}$, where P_{B_k} is the transmit power of the base station B_k, $d_{B_k,D_{a'}}$ is the distance from the base station B_k to DRU $D_{a'}$, and $h_{B_k,D_{a'}}$ is the channel gain of the link $l_{B_k,D_{a'}}$, which is of the exponential distribution with mean value 1 (i.e., $h_{B_k,D_{a'}} \sim \exp(1)$). Similarly, the interference power received at $D_{a'}$ is $I_{\mathbf{B}_{-k},D_{a'}} = \sum_{B_{k'}\in\mathbf{B}_{-k}} P_{B_{k'}}d_{B_{k'},D_{a'}}^{-\alpha}h_{B_{k'},D_{a'}}$, where $\mathbf{B}_{-k} = \mathbf{B} - \{B_k\}$, and the meanings of other notations are obvious.

Theorem 5: Under the PS architecture and in the cellular mode of D2D communications, for any D2D downlink $l_{B_k,D_{a'}}$, the energy harvested at $D_{a'}$ is given by Eq. (7).

Proof: See Appendix C. ■

2) EEH for Cellular Users: Note that energy harvesting for cellular users, which takes place over cellular downlinks, does not depend on any D2D communication mode (as D2D link is assumed to reuse uplink in cellular mode). Therefore, the energy harvested at a cellular user can be calculated in a similar fashion to that of a D2D user in cellular mode.

Theorem 6: Under the PS architecture, for any cellular downlink $l_{B_k,C_{\gamma,i}}$, the energy harvested at the cellular user $C_{\gamma,i}$ is specified by Eq. (7).

Proof: Follow the similar lines of Theorem 5's proof. ■

IV. Analysis of Ergodic Capacity

As stated before, a portion of time will be used for energy harvesting and the rest will be allocated for information decoding under the time switching (TS) architecture of SWIPT. The analysis of system capacity could be readily inherited from our previous results in [23], except that a time coefficient should be incorporated. Likewise, for the power splitting (PS) architecture of SWIPT a power coefficient needs to be associated with corresponding ergodic capacity in [23]. Thus, we skip the details and show the main results of ergodic capacity in the following.

A. Ergodic Capacity under TS Architecture

Given that the time allocated for information decoding under time switching architecture is $(1-\tau)T$, the ergodic capacity of D2D links and cellular links in all the three D2D communication modes, can be calculated as follows.

1) Ergodic Capacity in reuse mode: Suppose M is the spectrum available for cellular and D2D links. For any D2D link $l_{D_a,D_{a'}}$, its ergodic capacity would be

$$\mathrm{EC}_{D_a,D_{a'}} = (1-\tau)M\left(\sum_{n=1}^{\infty}\sum_{m=0}^{n-1}\sum_{b=1}^{n-m}(-1)^{n-m}J(m,n)\cdot \beta_b^{n-m}\frac{\pi\lambda_D\alpha}{2}I_b+\sum_{n=0}^{\infty}J(n,n)\frac{\alpha\pi\lambda_D}{2}I_0\right), \tag{8}$$

where $I_b = \int_0^{\infty}\frac{t^{b+\frac{\alpha}{2}-1}dt}{(\pi\lambda_D+t)^{b+1}\left(A^{\frac{\alpha}{2}}+t^{\frac{\alpha}{2}}\right)}$, $(b=0,1,\ldots)$, $A = \pi C(\alpha)\left(\sum_{j=1}^{s}\left(\frac{P_{C_j}}{P_D}\right)^{2/\alpha}\lambda_C+\lambda_D\right)$, $C(\alpha) = \frac{2\pi/\alpha}{\sin(2\pi/\alpha)}$, $\beta_b^{n-m} = \sum_{j=1}^{b}(-1)^j\binom{b}{j}\left(\frac{2j}{\alpha}\right)_{n-m}$, $(x)_k = x(x-1)\cdots(x-k+1)$, and $J(m,n) = \frac{K^n m!}{e^K}\binom{n}{m}\frac{1}{(n!)^2}$. For any cellular link $l_{C_{\gamma,i},B_k}$, its ergodic capacity is given by

$$\mathrm{EC}_{C_{\gamma,i},B_k} = \int_0^{\infty}\frac{(1-\tau)Mdt}{\frac{\lambda_C}{\lambda_B}\rho(e^t-1,\alpha)+C(\alpha)\frac{\lambda_D}{\lambda_B}\left(\frac{P_D(e^t-1)}{P_{C_\gamma}}\right)^{\frac{2}{\alpha}}+1}, \tag{9}$$

where $\rho(e^t-1,\alpha) = \sum_{j=1}^{s}\int_{\left(\frac{P_{C_\gamma}}{(e^t-1)P_{C_j}}\right)}^{\infty}\left(\frac{(e^t-1)P_{C_j}}{P_{C_\gamma}}\right)^{2/\alpha}\cdot\frac{1}{1+u^{\alpha/2}}du$, and P_{C_γ} is the transmit power of the cellular user $C_{\gamma,i}$.

2) Ergodic Capacity in dedicated mode: Suppose M_1 is the spectrum used by D2D links. For any D2D link $l_{D_a,D_{a'}}$, its ergodic capacity would be

$$\mathrm{EC}_{D_a,D_{a'}} = (1-\tau)M_1\left(\sum_{n=1}^{\infty}\sum_{m=0}^{n-1}\sum_{b=1}^{n-m}(-1)^{n-m}J(m,n)\cdot \beta_b^{n-m}\frac{\pi\lambda_D\alpha}{2}I_b+\sum_{n=0}^{\infty}J(n,n)\frac{\alpha\pi\lambda_D}{2}I_0\right), \tag{10}$$

where all notations have the same meanings as that in Eq. (8), except for $A = \pi C(\alpha)\lambda_D$ (which is part of I_b). Also, if $M_2 = M - M_1$ is the spectrum used by cellular users, then for any cellular link $l_{C_{\gamma,i},B_k}$, its ergodic capacity would be

$$\mathrm{EC}_{C_{\gamma,i},B_k} = \int_0^{\infty}\frac{(1-\tau)M_2dt}{1+\frac{\lambda_C}{\lambda_B}\rho(e^t-1,\alpha)}. \tag{11}$$

3) Ergodic Capacity in cellular mode: Suppose M_1 is the spectrum used by D2D links, for any D2D link $l_{D_a,D_{a'}}$, its ergodic capacity would be

$$\mathrm{EC}_{D_a,D_{a'}} = \frac{(1-\tau)M_1}{2}\int_0^{\infty}\mathrm{SP}_{D_a,D_{a'}}\left(e^t-1\right)dt, \tag{12}$$

where $\mathrm{SP}_{D_a,D_{a'}}$ is the success probability [23] of the D2D link $l_{D_a,D_{a'}}$. At the same time, suppose $M_2 = M - M_1$ is the

$$\mathrm{EEH}_{B_k,D_{a'}}(\text{or } \mathrm{EEH}_{B_k,C_{\gamma,i}}) = \kappa\eta\left\{P_{B_k}\left[\hat{d}^{-\alpha}(1-e^{-\pi\lambda_B\hat{d}^2})+(\pi\lambda_B)^{\alpha/2}\Gamma\left(\frac{-\alpha+2}{2},\pi\lambda_B\hat{d}^2\right)\right]+2\pi\lambda_B P_{B_{k'}}\cdot \left[\hat{d}^{-\alpha+2}(\tfrac{1}{2}+\tfrac{1}{\alpha-2})(1-e^{-\pi\lambda_B\hat{d}^2})+\tfrac{\hat{d}^{-\alpha}}{2\pi\lambda_B}\left[\left(\pi\lambda_B\hat{d}^2+1\right)e^{-\pi\lambda_B\hat{d}^2}-1\right]+\tfrac{1}{\alpha-2}(\pi\lambda_B)^{\frac{\alpha}{2}-1}\Gamma\left(\frac{-\alpha+4}{2},\pi\lambda_B\hat{d}^2\right)\right]\right\}. \quad (7)$$

spectrum used by cellular users. Then, for any cellular link $l_{C_{\gamma,i},B_k}$, its ergodic capacity would be

$$\mathrm{EC}_{C_{\gamma,i},B_k} = \int_0^\infty \frac{(1-\tau)M_2 dt}{1+\frac{\lambda_C}{\lambda_B}\rho\left(e^t-1,\alpha\right)}, \quad (13)$$

which is the same as the ergodic capacity in Eq. (11).

B. Ergodic Capacity under PS Architecture

Given that the power allocated for information decoding under the power splitting architecture is $(1-\kappa)P$, the ergodic capacity of D2D links and cellular links in the three D2D communication modes can be calculated in a similar fashion to that in TS architecture.

1) Ergodic Capacity in reuse mode: Suppose M is the spectrum used by cellular and D2D links. For any D2D link $l_{D_a,D_{a'}}$, its ergodic capacity would be

$$\mathrm{EC}_{D_a,D_{a'}} = (1-\kappa)M\left(\sum_{n=1}^{\infty}\sum_{m=0}^{n-1}\sum_{b=1}^{n-m}(-1)^{n-m}J\left(m,n\right)\cdot \beta_b^{n-m}\frac{\pi\lambda_D\alpha}{2}I_b+\sum_{n=0}^{\infty}J(n,n)\frac{\alpha\pi\lambda_D}{2}I_0\right), \quad (14)$$

which is essentially the same as the ergodic capacity in Eq. (8) (with τ replaced by κ). For any cellular link $l_{C_{\gamma,i},B_k}$, its ergodic capacity would be

$$\mathrm{EC}_{C_{\gamma,i},B_k} = \int_0^\infty \frac{(1-\kappa)M dt}{\frac{\lambda_C}{\lambda_B}\rho\left(e^t-1,\alpha\right)+C\left(\alpha\right)\frac{\lambda_D}{\lambda_B}\left(\frac{P_D(e^t-1)}{P_{C_\gamma}}\right)^{\frac{2}{\alpha}}+1}. \quad (15)$$

2) Ergodic Capacity in dedicated mode: Suppose M_1 and M_2 are the spectrums used by D2D links and cellular links, respectively. Then, for any D2D link $l_{D_a,D_{a'}}$, its ergodic capacity is given by

$$\mathrm{EC}_{D_a,D_{a'}} = (1-\kappa)M_1\left(\sum_{n=1}^{\infty}\sum_{m=0}^{n-1}\sum_{b=1}^{n-m}(-1)^{n-m}J\left(m,n\right)\cdot \beta_b^{n-m}\frac{\pi\lambda_D\alpha}{2}I_b+\sum_{n=0}^{\infty}J(n,n)\frac{\alpha\pi\lambda_D}{2}I_0\right), \quad (16)$$

which is basically the same as the ergodic capacity in Eq. (10), and for any cellular link $l_{C_{\gamma,i},B_k}$, its ergodic capacity would be

$$\mathrm{EC}_{C_{\gamma,i},B_k} = \int_0^\infty \frac{(1-\kappa)M_2 dt}{1+\frac{\lambda_C}{\lambda_B}\rho\left(e^t-1,\alpha\right)}. \quad (17)$$

Algorithm 1: Energy-efficient Mode Selection Mechanism

Input: λ_B, λ_C, λ_D, P_B , θ and α.
Output: communication mode.
for $(\mathrm{SIR} > \theta)$ **do**
  Calculate Ergodic Capacity, EEH according to Eq. (3–19),
  Obtain Δ_{EE} according to Eq. (20–21);
end
if $((\Delta_{EE_1} > \Delta_{EE_2})\&\&(\Delta_{EE_1} > \Delta_{EE_3}))$ **then**
  Select reuse mode;
else if $((\Delta_{EE_2} > \Delta_{EE_1})\&\&(\Delta_{EE_2} > \Delta_{EE_3}))$ **then**
  Select dedicated mode;
else
  Select cellular mode;
end

3) Ergodic Capacity in cellular mode: Let M_1 and M_2 be the spectrums used by D2D links and cellular links. Then, the ergodic capacity's of the D2D link $l_{D_a,D_{a'}}$ and the cellular link $l_{C_{\gamma,i},B_k}$ are

$$\mathrm{EC}_{D_a,D_{a'}} = \frac{(1-\kappa)M_1}{2}\int_0^\infty \mathrm{SP}_{D_a,D_{a'}}\left(e^t-1\right)dt \quad (18)$$

and

$$\mathrm{EC}_{C_{\gamma,i},B_k} = \int_0^\infty \frac{(1-\kappa)M_2 dt}{1+\frac{\lambda_C}{\lambda_B}\rho\left(e^t-1,\alpha\right)}, \quad (19)$$

respectively.

With the above expressions of EEH and ergodic capacity in hand, we are now in a position to design mode selection mechanism for D2D communications.

V. Energy Efficient Mode Selection Mechanism

In a general networks, energy efficiency in wireless networks can be defined as the ratio of the capacity to the total energy consumption of the network. In the process of computing system EE, the average power consumed by the circuit of mobile devices (P_{cir}) and the average power consumed by the base station (P_{cir_B}) need to be taken into account.

In the reuse and dedicated modes, suppose all cellular users are distributed over s tiers, P_{C_i} is the transmit power of cellular users at the i-th tier, and P_D is the transmit power

TABLE I: Simulation Parameters Setting

Parameter	Value
Number of tiers s	3
Transmit power of BSs (P_B)	20 w
Transmit power of cellular users on tier 1 (P_{C_1})	0.50 w
Transmit power of cellular users on tier 2 (P_{C_2})	1.00 w
Transmit power of cellular users on tier 3 (P_{C_3})	2.00 w
Transmit power of D2D users in reuse and dedicated modes (P_D)	0.25 w
Transmit power of D2D users on tier 1 in cellular mode (P_{D_1})	0.10 w
Transmit power of D2D users on tier 2 in cellular mode (P_{D_2})	0.20 w
Transmit power of D2D users on tier 3 in cellular mode (P_{D_3})	0.40 w
Density of BSs (λ_B)	$7 \cdot 10^{-6} m^{-2}$
Density of D2D users (λ_D)	$1 \cdot 10^{-4} m^{-2}$
Density of cellular users (λ_C)	$4 \cdot 10^{-5} m^{-2}$
Rician factor K	10
Average user device circuit power loss (P_{cir})	0.10 w
Average BS circuit power loss (P_{cir_B})	0.20 w
Total spectrum M	100 Hz
Bandwidth available for D2D users in dedicated and cellular modes M_1	50 Hz
Bandwidth available for cellular users in dedicated and cellular modes M_2	50 Hz
Energy harvesting allocation ratio under TS scheme τ	0.6
Energy harvesting allocation ratio under PS scheme κ	0.6
Energy conversion efficiency η	0.9
Path loss component α	4
Precision for short distance $\hat{d}$	1

of all D2D users. Then the EE of the entire system is given by

$$\Delta_{EE} = \frac{\lambda_C \sum_{i=1}^{s} \mathrm{EC}_{C_i} + \lambda_D \mathrm{EC}_D}{\lambda_C(\sum_{i=1}^{s} P_{C_i} + P_{cir} - \mathrm{EEH}_C) + \lambda_D(P_D + P_{cir} - \mathrm{EEH}_D)}, \quad (20)$$

where EC_{C_i} is the total ergodic capacity of cellular users at tier i, EC_D is the total ergodic capacity of D2D users, EEH_C is the total energy harvested by cellular users, and EEH_D is the total energy harvested by D2D users.

In the cellular mode, each D2D user acts just like a cellular user and the base station serves as a relay for D2D transmissions.Under these conditions, the EE of the entire system is given by Eq. (21), where EC_{D_i} is the total ergodic capacity of D2D users at tier i, and the meanings of other notations are the same as that in Eq. (20).

Once the computation of system EE is in place, we can eventually address the issue of mode selection for D2D communications - that is, which mode would be the best selection to conduct the D2D communications. One straightforward strategy would be to just choose the mode that will yield the best EE by Eqs. (20) and (21), as shown in Algorithm 1. But by doing so, it may not be able to ensure that the system ergodic capacity of the chosen mode would be optimal, for Eqs. (20) and (21) convey that an improved EE does not necessarily result from ergodic capacity. Another strategy, would be to first eliminate the modes that fail to deliver the systems ergodic capacity (i.e., greater than a predefined threshold) and then select the one that produces the best system EE from the remaining modes. This mechanism can be easily achieved by some minor modifications to Algorithm 1.

Note that the mode selection decision in this mechanism is made by the BS for each individual D2D link rather than for all D2D links simultaneously. As such, the proposed scheme doesn't need perfect synchronization of all users.

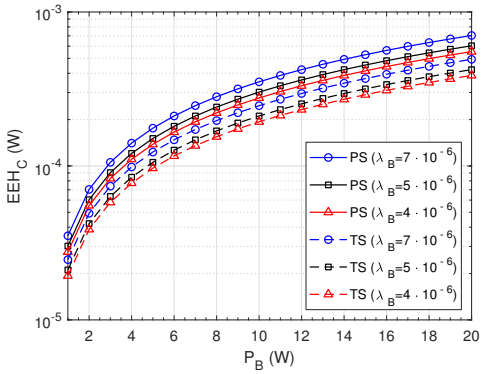

Fig. 4: Relation between energy harvested by a single cellular user and P_B (PS = power splitting, TS = time switching).

VI. Simulation Results

In this section, we carry out extensive simulations to access the energy harvested by cellular and D2D users as well as the system EE, in the presence of SWIPT under the reuse, dedicated, and cellular mode of D2D communications, respectively. The results of these simulations are subsequently analyzed. All simulation parameters (which are similar to that in [23]) and their values, unless otherwise specified, are listed in Table I. Note that s is set to 3, it can also be 4, 5, or other values. The simulation results deliver the same insights even s takes another value.

Fig. 4 depicts the relation of the energy harvested by a single cellular user with the transmit power; P_B and the density; λ_B of the base station; B, respectively. It can be clearly observed that the EEH increases when P_B or λ_B increases. This is not surprising as an increase in P_B will result in an increase in the received useful signals, and an increase in λ_B will result in an increase in interference signals for cellular users. Since both useful and interference signals are used in SWIPT, we consequently see an increase in the harvested energy. Also, note that cellular users can only harvest energy from the base station under the TS architecture. Moreover, from Fig. 4, we can see a higher value of the harvest energy from both base station and inference signals under the PS architecture. The reason for EEH_C in the PS architecture being higher than that in the TS one is that: given the same value to τ and κ, the cellular users can collect energy from both of the BS and the interference in the former architecture, but cellular user can harvest energy only from the BS in the later one.

Fig. 5, on the other hand, shows the energy harvested by a single D2D user with respect to the average transmit power; P_D and the density; λ_D of D2D users, under the reuse,

$$\Delta_{EE} = \frac{\lambda_C \sum_{i=1}^{s} \mathrm{EC}_{C_i} + \lambda_D \sum_{i=1}^{s} \mathrm{EC}_{D_i}}{\lambda_C(\sum_{i=1}^{s} P_{C_i} + P_{cir} - \mathrm{EEH}_C) + \lambda_D(\sum_{i=1}^{s} P_{D_i} + P_{cir} + P_{cir\_B} + P_B - \mathrm{EEH}_D)}. \quad (21)$$

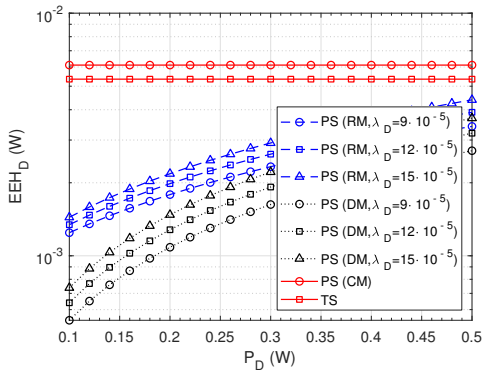

Fig. 5: Relation between energy harvested by a single D2D user and P_D (RM = reuse mode, DM = dedicated mode, CM = cellular mode).

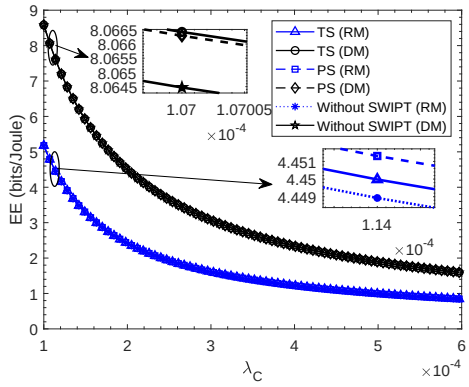

Fig. 6: Relation between system EE and λ_C in reuse and dedicated modes.

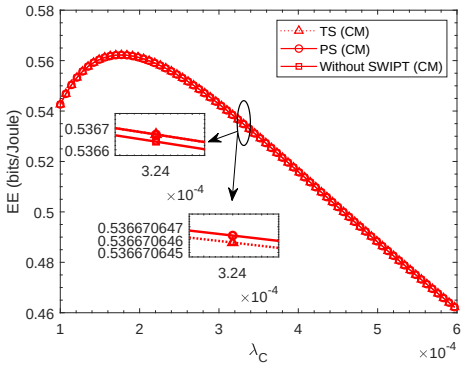

Fig. 7: Relation between system EE and λ_C and in cellular mode.

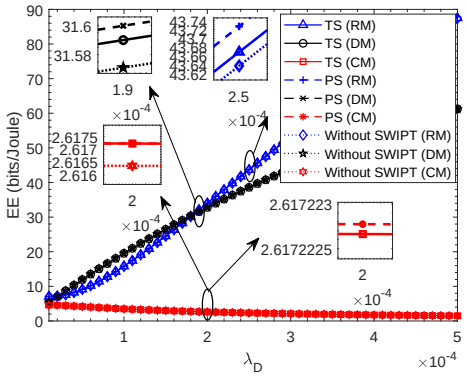

Fig. 8: Relation between system EE and λ_D under the TS and PS architectures and w.r.t. the 3 D2D communication modes.

dedicated, and cellular modes, respectively. [1] This indicates that with the PS architecture, the amount of energy harvested by a D2D receiver, in terms of the communication mode, has the following rank: cellular mode $>$ reuse mode $>$ dedicated mode. This is due to the fact that in cellular mode the energy harvested by D2D receivers directly comes from the base station, which has nothing to do with P_D and λ_D. More specifically, the base station has much greater transmit power than that of D2D transmitters, and the interference experienced at the D2D receivers in dedicated mode is less than that in reuse mode. As for the relation between the harvested energy and the density of D2D users, an increase in λ_D will cause an increase in the amount of received signals at a D2D receiver. Finally, since the harvested energy by a D2D receiver under the TS architecture comes solely from the base station, it is independent of the transmit power or the density of D2D users (see a straight line Fig. 5).

Figs. 6 and 7 depict the relations between the system EE and the cellular user density λ_C under the three different communication modes. In particular, Fig. 6 reveals that the system EE decreases as the λ_C increases in the reuse and dedicated modes in both TS and PS architectures. Nonetheless, the system EE in dedicated mode is higher than that in reuse mode. This behavior can be explained by the following facts: In reuse mode, an increase in λ_C will cause an increase in interference between D2D users and cellular users, causing a decrease in the ergodic capacity for both D2D and cellular links. The system EE thus decreases, as observed. In the dedicated mode, however, there is no interference between D2D and cellular links. As such, an increase in λ_C will only cause an increase in interference between cellular users. Consequently, the system EE in dedicated mode is higher

[1] Strictly speaking, the transmit power of D2D links in cellular mode is denoted by P_{D_γ} (not P_D) where γ is the tier on which the D2D user is located. But, since the energy harvested by D2D users in cellular mode does not depend on the transmit power of D2D links, here we use P_D to collectively denote the transmit power of D2D links (in all modes) as doing so will not affect the outcomes.

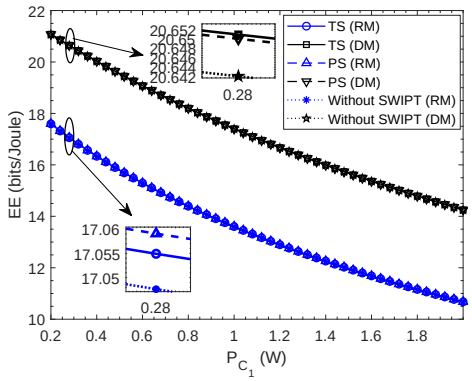

Fig. 9: Relation between system EE and P_{C_1} under the TS and PS architectures and w.r.t. reuse and dedicated modes.

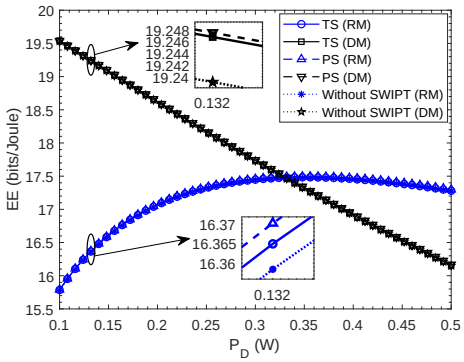

Fig. 11: Relation between system EE and P_D under the TS and PS architectures and w.r.t. reuse and dedicated modes.

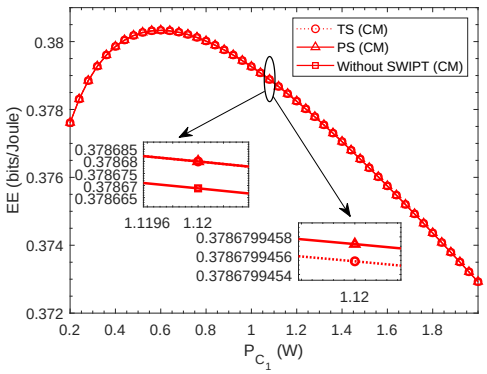

Fig. 10: Relation between system EE and P_{C_1} under the TS and PS architectures and w.r.t. cellular mode.

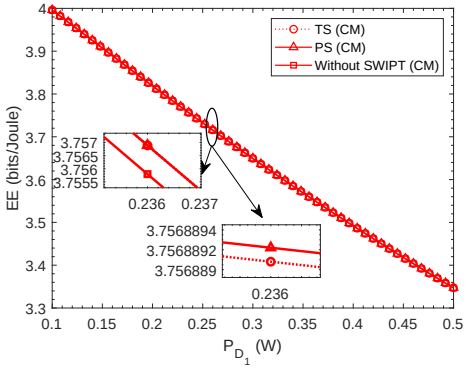

Fig. 12: Relation between system EE and P_{D_1} under the TS and PS architectures and w.r.t. cellular mode.

than that in reuse mode. On the other hand, Fig. 7 shows that the system EE under the cellular mode increases first and then starts to drop as the λ_C increases. Bear in mind that when the density of cellular users is low, the energy consumption of D2D users via the data relay at the base station dominates the energy consumption of cellular users. At the same time, any (small) increase in λ_C increases both the energy consumption and the ergodic capacity for cellular users, but the latter increase would be relatively more substantial. As a result, we see an increase of the system EE when λ_C is small. However, when λ_C gets much larger and keeps growing, the system starts having a shortage of spectrum resources. Under these conditions, the energy consumption of cellular devices will dominate the total energy consumption and become a major factor with regards to ergodic capacity and energy consumption of the system. Consequently, we see a decrease in system EE as the density of cellular users becomes sufficiently large. Combining Figs. 6 and 7, we see that the system EE has the following rank in terms of the D2D communication mode: dedicated mode $>$ reuse mode $>$ cellular mode. Finally, note that these two figures show that the system EE can be improved with SWIPT, especially for D2D communications in reuse mode in the context of ultra-dense cellular network (larger λ_B, λ_C, λ_D lead to higher EE), compared with [23].

Fig. 8 depicts the relation between the system EE and the density λ_D of D2D users under the TS and PS architectures and with respect to the three D2D communication modes. It can be seen that under both TS and PS architectures, the system EE increases as λ_D increases in both reuse and dedicated modes, but decreases in cellular mode. This is mainly due to the fact that in the reuse and dedicated modes, the total ergodic capacity of the system will increase as the density of D2D users increases [23], but the total energy consumption of the system remains roughly unchanged. This, by Eq. (20), will subsequently lead to an increase in the system EE. However, in cellular mode, the base station needs to serve as a relay node for D2D communications. Since the base station consumes a great deal of energy in transferring data for D2D communications, and the ergodic capacity of D2D links is substantially smaller when compared with cellular links, the system EE tends to decrease as λ_D increases. From Fig. 8, we can see that when the D2D user density λ_D is relatively low, the system energy efficiency is higher in dedicated mode. On the contrary, when λ_D exceeds a certain range, the system energy efficiency is higher in dedicated mode.

The relation between the system EE and the cellular transmit power P_{C_1} at the first tier under the TS and PS architecture and with respect to the three D2D communication modes is shown in Figs. 9 and 10. Obviously, Fig. 9 indicates that the system EE decreases as the P_{C_1} increases in both reuse and dedicated modes and under both TS and PS architectures. Such behavior is due to a fact that an increase in P_{C_1} will cause either higher interference between D2D users and cellular

users (and thus lower ergodic capacity of the system), or higher energy consumption of the system, or both. This will inevitably cause a decrease in the system EE. Fig. 10, on the other hand, reveals that the system EE initially increases slowly and then decreases slowly as the P_{C_1} increases in cellular mode and under both TS and PS architectures. The reason for such behavior is that when P_{C_1} is small and grows within a certain range, it will cause an increase in the ergodic capacity of cellular users. Therefore, we see a slow increase in system EE initially. However, when P_{C_1} keeps growing and becomes relatively large, it will cause an excessive increase in the cellular energy consumption in the system, which will consequently bring the system EE down.

Figs. 11 and 12 depict the relation between the system EE and transmit power of D2D users (P_D) or the transmit power of D2D users at the first tier (P_{D_1}) under the TS and PS architectures. The reasons for the fact that as P_D or P_{D_1} increases the system EE increases first and then decreases in reuse mode (also, decreases straightforwardly in both dedicated and cellular modes) can be explained as follows. In the reuse mode, the distance from a D2D transmitter to its receiver is typically short. Therefore, the interference experienced at D2D receivers, when P_D is small and increases within a certain range, can be roughly ignored. Consequently, this will boost the ergodic capacity of D2D users, which in turn can result in an increase in the system EE. On the other hand, when P_D grows notably high the ensuing interference it causes will be substantially stronger, leading to a decrease in ergodic capacity and a decrease in EE as well. In the dedicated mode, there is no interference between D2D users and cellular users. In this case, an increase in P_D will cause a decrease in the ergodic capacity and an increase in energy consumption for D2D users. As a result, the system EE decreases as the P_D increases. The situation in cellular mode (Fig. 12) can be explained in a similar fashion, with P_{D_1} perceived as P_D.

VII. Conclusion

In this paper, we have studied the energy-efficient SWIPT-empowered mode selection in D2D communications. Under the TS and PS architectures of SWIPT, we have analyzed the energy harvested by D2D users and cellular users using stochastic geometry, and have obtained the closed-form expression of the ergodic energy-harvested (EEH). Armed with EEH and the results of ergodic capacity, we have designed a mode selection mechanism based on the system EE. We have also conducted numerous simulations to verify the effectiveness of the proposed mechanism. The simulation results show that our mechanism is able to select the best mode for D2D communication with better EE, especially in an ultra-dense cellular network, compared with a state-of-the-art mode selection approach.

References

[1] S. Shamaei, S. Bayat, and A. M. A. Hemmatyar, "Interference management in d2d-enabled heterogeneous cellular networks using matching theory," *IEEE Transactions on Mobile Computing*, pp. 1–1, 2018.

[2] J. Liu, H. Nishiyama, N. Kato, and J. Guo, "On the outage probability of device-to-device-communication-enabled multichannel cellular networks: An rss-threshold-based perspective," *IEEE Journal on Selected Areas in Communications*, vol. 34, no. 1, pp. 163–175, Jan 2016.

[3] A. Salem, C. Masouros, and K. Wong, "Sum rate and fairness analysis for the mu-mimo downlink under psk signalling: Interference suppression vs exploitation," *IEEE Transactions on Communications*, pp. 1–1, 2019.

[4] A. Omri and M. O. Hasna, "Modeling and performance analysis of 3-d heterogeneous networks with interference management," *IEEE Communications Letters*, vol. 21, no. 8, pp. 1787–1790, Aug 2017.

[5] J. Kim, S. Kim, J. Bang, and D. Hong, "Adaptive mode selection in d2d communications considering the bursty traffic model," *IEEE Communications Letters*, vol. 20, no. 4, pp. 712–715, April 2016.

[6] D. Della Penda, L. Fu, and M. Johansson, "Mode selection for energy efficient d2d communications in dynamic tdd systems," in *2015 IEEE International Conference on Communications (ICC)*, June 2015, pp. 5404–5409.

[7] J. Liu, N. Kato, J. Ma, and N. Kadowaki, "Device-to-device communication in lte-advanced networks: A survey," *IEEE Communications Surveys Tutorials*, vol. 17, no. 4, pp. 1923–1940, Fourthquarter 2015.

[8] Y. Zhang, Y. Shen, X. Jiang, and S. Kasahara, "Mode selection and spectrum partition for d2d inband communications: A physical layer security perspective," *IEEE Transactions on Communications*, vol. 67, no. 1, pp. 623–638, Jan 2019.

[9] Y. Xu and S. Wang, "Mode selection for energy efficient content delivery in cellular networks," *IEEE Communications Letters*, vol. 20, no. 4, pp. 728–731, April 2016.

[10] Y. Lu, K. Xiong, P. Fan, Z. Ding, Z. Zhong, and K. B. Letaief, "Global energy efficiency in secure miso swipt systems with non-linear power-splitting eh model," *IEEE Journal on Selected Areas in Communications*, vol. 37, no. 1, pp. 216–232, Jan 2019.

[11] Y. Yuan, Y. Xu, Z. Yang, P. Xu, and Z. Ding, "Energy efficiency optimization in full-duplex user-aided cooperative swipt noma systems," *IEEE Transactions on Communications*, pp. 1–1, 2019.

[12] J. Huang, C. Xing, and C. Wang, "Simultaneous wireless information and power transfer: Technologies, applications, and research challenges," *IEEE Communications Magazine*, vol. 55, no. 11, pp. 26–32, Nov 2017.

[13] R. Atat, L. Liu, N. Mastronarde, and Y. Yi, "Energy harvesting-based d2d-assisted machine-type communications," *IEEE Transactions on Communications*, vol. 65, no. 3, pp. 1289–1302, March 2017.

[14] J. Huang, C. Xing, and M. Guizani, "Power allocation for d2d communications with swipt," *IEEE Transactions on Wireless Communications*, pp. 1–1, 2020.

[15] A. El Shafie, K. Tourki, and N. Al-Dhahir, "An artificial-noise-aided hybrid ts/ps scheme for ofdm-based swipt systems," *IEEE Communications Letters*, vol. 21, no. 3, pp. 632–635, March 2017.

[16] P. Liu, S. Gazor, I. Kim, and D. I. Kim, "Energy harvesting noncoherent cooperative communications," *IEEE Transactions on Wireless Communications*, vol. 14, no. 12, pp. 6722–6737, Dec 2015.

[17] M. M. Deshmukh, S. M. Zafaruddin, A. Mihovska, and R. Prasad, "Stochastic-geometry based characterization of aggregate interference in tvws cognitive radio networks," *IEEE Systems Journal*, pp. 1–4, 2019.

[18] J. Liu, Y. Kawamoto, H. Nishiyama, N. Kato, and N. Kadowaki, "Device-to-device communications achieve efficient load balancing in lte-advanced networks," *IEEE Wireless Communications*, vol. 21, no. 2, pp. 57–65, April 2014.

[19] J. Huang, Y. Zhou, Z. Ning, and H. Gharavi, "Wireless power transfer and energy harvesting: Current status and future prospects," *IEEE Wireless Communications*, pp. 1–7, 2019.

[20] A. H. Sakr and E. Hossain, "Cognitive and energy harvesting-based d2d communication in cellular networks: Stochastic geometry modeling and analysis," *IEEE Transactions on Communications*, vol. 63, no. 5, pp. 1867–1880, May 2015.

[21] R. Atat, L. Liu, N. Mastronarde, and Y. Yi, "Energy harvesting-based d2d-assisted machine-type communications," *IEEE Transactions on Communications*, vol. 65, no. 3, pp. 1289–1302, March 2017.

[22] Z. Kuang, G. Liu, G. Li, and X. Deng, "Energy efficient resource allocation algorithm in energy harvesting-based d2d heterogeneous networks," *IEEE Internet of Things Journal*, vol. 6, no. 1, pp. 557–567, Feb 2019.

[23] J. Huang, J. Zou, and C. Xing, "Energy-efficient mode selection for d2d communications in cellular networks," *IEEE Transactions on Cognitive Communications and Networking*, vol. 4, no. 4, pp. 869–882, Dec 2018.

[24] L. Mohjazi, S. Muhaidat, M. Dianati, and M. Al-Qutayri, "Outage probability and throughput of swipt relay networks with differential modulation," in *2017 IEEE 86th Vehicular Technology Conference (VTC-Fall)*, Sep. 2017, pp. 1–6.

APPENDIX A
PROOF OF THEOREM 1

Note that

$$\mathrm{EEH}_{B_k,D_{a'}} = E[S_D] = P_{B_k} E[d_{B_k,D_{a'}}^{-\alpha} h_{B_k,D_{a'}}] = P_{B_k} E[d_{B_k,D_{a'}}^{-\alpha}],$$

and

$$E[d_{B_k,D_{a'}}^{-\alpha}] = \int_0^{\infty} d_{B_k,D_{a'}}^{-\alpha} \cdot 2\pi\lambda_B d_{B_k,D_{a'}} \exp(-\pi\lambda_B d_{B_k,D_{a'}}^2) dd_{B_k,D_{a'}},$$

where $\hat{d} \geq 1$ is used to avoid model inaccuracy for very short distance [27], [31]. Specifically, when $d_{B_k,D_{a'}} < \hat{d}$, the path loss is $\hat{d}^{-\alpha}$; when $d_{B_k,D_{a'}} > \hat{d}$, the path loss is $d_{B_k,D_{a'}}^{-\alpha}$. Thus,

$$\begin{aligned} E[d_{B_k,D_{a'}}^{-\alpha}] &= \int_0^{\hat{d}} \hat{d}^{-\alpha} \cdot 2\pi\lambda_B d_{B_k,D_{a'}} \exp(-\pi\lambda_B d_{B_k,D_{a'}}^2) dd_{D_{a,a'}} + \int_{\hat{d}}^{\infty} d_{B_k,D_{a'}}^{-\alpha} \cdot 2\pi\lambda_B d_{B_k,D_{a'}} \exp(-\pi\lambda_B d_{B_k,D_{a'}}^2) dd_{B_k,D_{a'}} \\ &= \hat{d}^{-\alpha} \left(-e^{-\pi\lambda_B \hat{d}^2} + 1\right) + (\pi\lambda_B)^{\alpha/2} \Gamma\left(\frac{-\alpha+2}{2}, \pi\lambda_B \hat{d}^2\right) \end{aligned}$$

and the theorem follows.

APPENDIX B
PROOF OF THEOREM 3

Note that

$$\begin{aligned} E\left(S_D + I\right) &= P_D E\left(d_{D_a,D_{a'}}^{-\alpha} g_{D_a,D_{a'}}\right) + E\left(I_{\mathbf{C},D_{a'}}\right) + E\left(I_{\mathbf{D}_{-a},D_{a'}}\right), \\ E\left(d_{D_a,D_{a'}}^{-\alpha} g_{D_a,D_{a'}}\right) &= E\left(d_{D_a,D_{a'}}^{-\alpha}\right) \cdot E\left(g_{D_a,D_{a'}}\right), \end{aligned}$$

$$\begin{aligned} E\left(d_{D_a,D_{a'}}^{-\alpha}\right) &= \int_0^{\hat{d}} \hat{d}^{-\alpha} 2\pi\lambda_D d_{D_a,D_{a'}} \exp(-\pi\lambda_D d_{D_a,D_{a'}}^2) dd_{D_a,D_{a'}} + \int_{\hat{d}}^{\infty} d_{D_a,D_{a'}}^{-\alpha} 2\pi\lambda_D d_{D_a,D_a} \exp(-\pi\lambda_D d_{D_a,D_{a'}}^2) dd_{D_a,D_{a'}} \\ &= \hat{d}^{-\alpha} \left(-e^{-\pi\lambda_D \hat{d}^2} + 1\right) + (\pi\lambda_D)^{\alpha/2} \Gamma\left(\frac{-\alpha+2}{2}, \pi\lambda_D \hat{d}^2\right), \\ E\left(g_{D_a,D_{a'}}\right) &= \int_0^{\infty} g_{D_a,D_{a'}} \exp\left(-K - g_{D_a,D_{a'}}\right) \sum_{k=0}^{\infty} \frac{\left(K g_{D_a,D_{a'}}\right)^k}{(k!)^2} dg_{D_a,D_{a'}} \\ &= \sum_{k=0}^{\infty} \exp\left(-K\right) \frac{K^k}{(k!)^2} \int_0^{\infty} {g_{D_a,D_{a'}}}^{k+1} \exp\left(-g_{D_a,D_{a'}}\right) dg_{D_a,D_{a'}} \\ &= \sum_{k=0}^{\infty} \exp\left(-K\right) \frac{K^k}{(k!)^2} \cdot (k+1)! = \exp\left(-K\right) \left(\sum_{k=0}^{\infty} \frac{K^k (k+1)}{k!}\right) = 1 + K, \end{aligned}$$

$$\begin{aligned} E\left(I_{\mathbf{C},D_{a'}}\right) &= E\left(\sum_{j=1}^{s} \sum_{C_{j,i} \in \mathbf{C}} P_{C_j} d_{C_{j,i},D_{a'}}^{-\alpha} h_{C_{j,i},D_{a'}}\right) = \sum_{j=1}^{s} P_{C_j} E\left(\sum_{\substack{C_{j,i} \in \mathbf{C} \\ d_{C_{j,i},D_{a'}} > d}} d_{C_{j,i},D_{a'}}^{-\alpha} + \sum_{\substack{C_{j,i} \in \mathbf{C} \\ d_{C_{j,i},D_{a'}} < d}} d_{C_{j,i},D_{a'}}^{-\alpha}\right) \\ &= \sum_{j=1}^{s} P_{C_j} \cdot \left(2\pi\lambda_C \int_{\hat{d}}^{\infty} d_{C_{j,i},D_{a'}}^{-\alpha} \cdot d_{C_{j,i},D_{a'}} dd_{C_{j,i},D_{a'}} + \int_0^{\hat{d}} \hat{d}^{-\alpha} d_{C_{j,i},D_{a'}} dd_{C_{j,i},D_{a'}}\right) \\ &= \sum_{j=1}^{s} P_{C_j} \pi\lambda_C \hat{d}^{-\alpha+2} \frac{\alpha}{\alpha-2}, \end{aligned}$$

and $E\left(I_{\mathbf{D}_{-a},D_{a'}}\right) = P_D \pi\lambda_D \hat{d}^{-\alpha+2} \frac{\alpha}{\alpha-2}$.

Thus,

$$\begin{aligned}E\left(S_D+I\right)&=E\left(P_D d_{D_a,D_{a'}}^{-\alpha}g_{D_a,D_{a'}}\right)+E\left(I_{\mathbf{C},D_{a'}}\right)+E\left(I_{\mathbf{D}_{-a},D_{a'}}\right)\\&=P_D\left[\hat{d}^{-\alpha}\left(-e^{-\pi\lambda_D\hat{d}^2}+1\right)+(\pi\lambda_D)^{\alpha/2}\Gamma\left(\frac{-\alpha+2}{2},\pi\lambda_D\hat{d}^2\right)\right](1+K)+\sum_{j=1}^{s}P_{C_j}\pi\lambda_C\hat{d}^{-\alpha+2}\frac{\alpha}{\alpha-2}\\&+P_D\pi\lambda_D\hat{d}^{-\alpha+2}\frac{\alpha}{\alpha-2}.\end{aligned}$$

APPENDIX C
PROOF OF THEOREM 5

The computation of $E(S_D)$ is similar to that in Theorem 1. Also, note the following computation

$$\begin{aligned}E\left(I_{\mathbf{B}_{-k},D_{a'}}\right)&=E_{\mathbf{B},h}\left(\sum_{B_{k'}\in\mathbf{B}_{-k}}P_{B_{k'}}d_{B_{k'},D_{a'}}^{-\alpha}h_{B_{k'},D_{a'}}\right)=E_{\mathbf{B}}\left(\sum_{B_{k'}\in\mathbf{B}_{-k}}P_{B_{k'}}d_{B_{k'},D_{a'}}^{-\alpha}\right)\\&=2\pi\lambda_B P_{B_{k'}}\int_0^{\infty}\left[\int_{d_{B_{k'},D_{a'}}}^{\infty}\left[\max(d_{B_{k'},D_{a'}},d)\right]^{-\alpha}d_{B_{k'},D_{a'}}dd_{B_{k'},D_{a'}}\right]f_{D_{B_{k'},D_{a'}}}\left(d_{B_{k'},D_{a'}}\right)dd_{B_{k'},D_{a'}}\\&=2\pi\lambda_B P_{B_{k'}}\left[\int_0^{\hat{d}}\left(\int_{d_D}^{\hat{d}}d_{B_{k'},D_{a'}}\cdot\hat{d}^{-\alpha}dd_{B_{k'},D_{a'}}+\int_{\hat{d}}^{\infty}d_{B_{k'},D_{a'}}\cdot d_{B_{k'},D_{a'}}^{-\alpha}dd_{B_{k'},D_{a'}}\right)2\pi\lambda_B d_D\exp(-\pi\lambda_B d_D^2)dd_D\right.\\&\left.+\int_{\hat{d}}^{\infty}\left(\int_{d_D}^{\infty}d_{B_{k'},D_{a'}}\cdot {d_{B_{k'},D_{a'}}}^{-\alpha}dd_{B_{k'},D_{a'}}\right)2\pi\lambda_B d_D\exp(-\pi\lambda_B d_D^2)dd_D\right]\\&=2\pi\lambda_B P_{B_{k'}}\left[\hat{d}^{-\alpha+2}\frac{\alpha}{2(\alpha-2)}\left(1-e^{-\pi\lambda_B\hat{d}^2}\right)+\frac{1}{2\pi\lambda_B}\hat{d}^{-\alpha}\left[\left(\pi\lambda_B\hat{d}^2+1\right)e^{-\pi\lambda_B\hat{d}^2}-1\right]+\frac{1}{\alpha-2}(\pi\lambda_B)^{\frac{\alpha}{2}-1}\right.\\&\left.\cdot\Gamma\left(\frac{-\alpha+4}{2},\pi\lambda_B\hat{d}^2\right)\right].\end{aligned}$$

By combining these two parts, the proof of the theorem is complete.

[25] ——, "Performance analysis of swipt relay networks with noncoherent modulation," *IEEE Transactions on Green Communications and Networking*, vol. 2, no. 4, pp. 1072–1086, Dec 2018.

[26] S. K. Zaidi, S. F. Hasan, and X. Gui, "Time switching based relaying for coordinated transmission using noma," in *2018 Eleventh International Conference on Mobile Computing and Ubiquitous Network (ICMU)*, Oct 2018, pp. 1–5.

[27] T. A. Zewde and M. C. Gursoy, "Energy efficiency analysis for wireless-powered cellular networks," in *2017 51st Annual Conference on Information Sciences and Systems (CISS)*, March 2017, pp. 1–6.

[28] Z. Zhou, M. Peng, and Z. Zhao, "Joint data-energy beamforming and traffic offloading in cloud radio access networks with energy harvesting-aided d2d communications," *IEEE Transactions on Wireless Communications*, vol. 17, no. 12, pp. 8094–8107, Dec 2018.

[29] H. Wu, X. Tao, N. Zhang, D. Wang, S. Zhang, and X. Shen, "On base station coordination in cache- and energy harvesting-enabled hetnets: A stochastic geometry study," *IEEE Transactions on Communications*, vol. 66, no. 7, pp. 3079–3091, July 2018.

[30] T. A. Khan, P. V. Orlik, K. J. Kim, R. W. Heath, and K. Sawa, "A stochastic geometry analysis of large-scale cooperative wireless networks powered by energy harvesting," *IEEE Transactions on Communications*, vol. 65, no. 8, pp. 3343–3358, Aug 2017.

[31] K. Huang and V. K. N. Lau, "Enabling wireless power transfer in cellular networks: Architecture, modeling and deployment," *IEEE Transactions on Wireless Communications*, vol. 13, no. 2, pp. 902–912, February 2014.